Extended Abstracts of the 2001 International Conference on Solid State Devices and Materials, Tokyo, 2001, pp. 178–179

**A-5-1**

# Ultrathin Nitrided-Nanolaminate ($Al_2O_3/ZrO_2/Al_2O_3$) for Gate Dielectrics Application

S. Jeon, H. Yang, H. Chang, D. G. Park[1], K. Y. Lim[1], In-Seok Yeo,[1] H. Koh[2], H. W. Yeom[2], and Hyunsang Hwang

Department of Materials Science and Engineering, Kwangju Institute of Science and Technology
#1, Oryong-dong, Puk-gu, Kwangju, 500-712, KOREA
Phone:+82-62-970-2314 Fax:+82-62-970-2304 E-mail: hwanghs@ kjist.ac.kr
[1]Advanced Process Team, Memory R&D Div., Hynix Semiconductor, Inc., Ichon, Kyoungki, 467-701, KOREA
[2] Atomic-scale Surface Science Research Center, Institute of Physics&Applied Physics, Yonsei University, 120-749, KOREA

## 1. Introduction

The $ZrO_2$ film represents a promising alternative gate dielectric because it exhibits a high permittivity of 25, compatibility with silicon substrate without any barrier layer [1]. However, there are some potential concerns about low temperature crystallization, as well as the degradation of equivalent oxide thickness due to the increase in thickness and the formation of silicate at high temperatures. To improve the thermal stability of $ZrO_2$, we investigated nanolaminate ($Al_2O_3/ZrO_2/Al_2O_3$).

## 2. Experimentals

Nanolaminate ($Al_2O_3/ZrO_2/Al_2O_3$) was deposited by atomic layer deposition. To improve thermal stability, remote plasma nitridation in $N_2$ was performed. After the deposition of a 150nm-thick layer of Pt, MOS devices with a gate area of $9\times10^{-6}$ $cm^2$ were defined by photolithography and etching. For comparison, $n^+$ doped polysilicon was deposited at 560°C and activation anneal was performed at 700°C for 10min.

## 3. Results & Discussion

Fig. 1 shows typical C-V and I-V characteristics of MOS capacitors with nanolaminate dielectrics. The effective oxide thickness which include quantum mechanical effects and the leakage current at 1V below flatband voltage were 10.3Å and $3\times10^{-4}$ A/$cm^2$, respectively. The physical thickness was approximately 4.7nm including 0.6nm-thick interfacial layer as shown in Fig. 2. Fig. 3 shows medium-energy ion scattering (MEIS) spectroscopy result. Based on simulation, we confirmed the stoichiometric $Al_2O_3$ and $ZrO_2$ layer. In addition, 5Å-thick $Zr_{0.33}Al_{0.1}O_{0.57}$ layer and 5Å-thick $Al_{0.1}Si_{0.3}O_{0.6}$ were also found at the interface. Based on XPS analysis, we confirmed Al, Zr and O peak in nanolaminate.

To evaluate the bandgap of nanolaminate, we performed XPS analysis as shown in Fig. 4. $E_F$-$E_V$ of $Al_2O_3$ and $ZrO_2$ was extracted from Fig. 4(a). $E_C$-$E_F$ was extracted from the value of XAS-binding energy as shown in Fig. 4(b). The estimated bandgap of $Al_2O_3$ and $ZrO_2$ was 7.9eV and 6.1eV, respectively as shown in Fig. 5.

The leakage current mechanism of nanolaminate was evaluated as shown in Fig. 7-10. The applied electric field of each layer was calculated as shown in Fig. 7. It was reported that PLD-$ZrO_2$ exhibits Poole-Frenkel conduction [2]. Considering negligible temperature dependence as shown in Fig. 8 and field dependence as shown in Fig. 9, the trap assisted tunneling through $ZrO_2$ and direct tunneling through $Al_2O_3$ can explain the I-V characteristics of nanolaminate. As shown in Fig. 10, Poole-Frenkel fitting cannot explain I-V results. Without $Al_2O_3$-layer, the leakage current was significantly high.

Compared with Pt gate, MOS capacitors with polysilicon gate electrode shows lower capacitance values as shown in Fig. 11. The growth of interfacial oxide layer during the activation annealing at 700°C for 10min can explain the degradation of capacitance. To minimize the degradation of capacitance, we have performed plasma nitridation in $N_2$ ambient. Based on AFM analysis, the surface roughness after nitridation is almost negligible. The plasma nitridation of nanolaminate significantly reduces the degradation of capacitance characteristics as shown in Fig 12. Fig. 13 shows leakage current characteristics of both samples with polysilicon gate. Although the capacitance value of nitrided sample is higher, the leakage current was slightly lower for nitrided sample which can be explained by lower trap concentration of nitrided sample [3]. The effect of nitridation on bandgap of both $Al_2O_3$ and $ZrO_2$ was negligible which was confirmed by XPS analysis. As shown in Fig. 14, the interfacial oxide growth which was confirmed by the silicon oxide or silicate peak at 102eV in Si2p spectra was significantly low for nitrided samples.

## 4. Summary

The excellent electrical characteristics of nanolaminate have been investigated. By employing plasma nitridation process, a significant improvement of thermal stability was observed. The improvement can be explained by reduction of interfacial oxide formation during high temperature process.

## Acknowledgments

Authors thank to Mr. C. Werkhoven of ASM America for nanolaminate sample preparation. This work was supported by National Program for Tera Level Nano Devices through MOST.

## References

[1] C. Lee et al., *Tech. Dig. IEDM*, 27 (2000)
[2] T. Yamaguchi et al., *Tech. Dig. IEDM*, 19 (2000)
[3] G. B. Alers, Appl. Phys. Lett., 72, 1308 (1998)

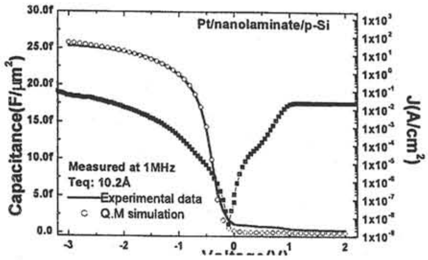


Fig 1. C-V & J-V of nanolaminate

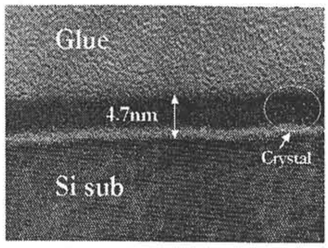


Fig 2. XTEM results nanolaminate/p-Si

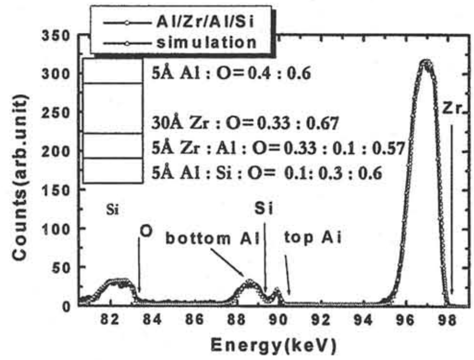


Fig 3. MEIS data of nanolaminate

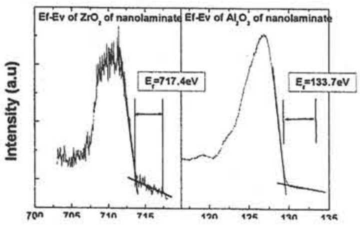


Fig 4.(a) XPS data of nanolaminate

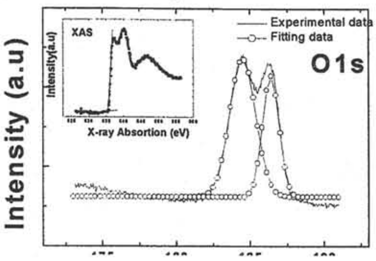


Fig 4(b) O1s spectra of nanolaminate

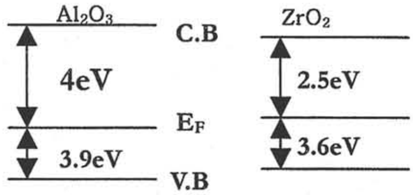


Fig 5 The bandgap information

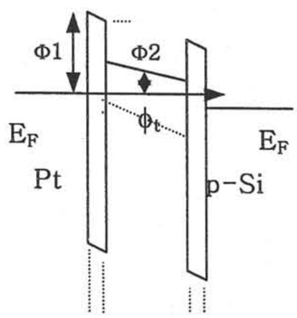


Fig 6. The band diagram of Pt/nanolaminate /p-Si

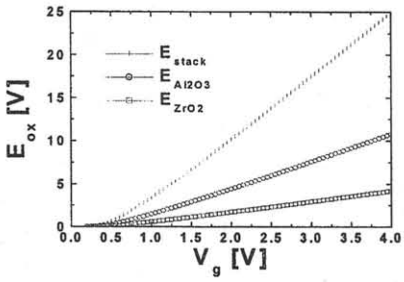


Fig 7. The calculated electric field. Total, $Al_2O_3$, $ZrO_2$

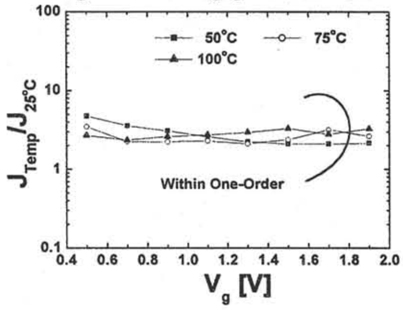


Fig 8. The normalized current density with temperature, which shows insensitivity.

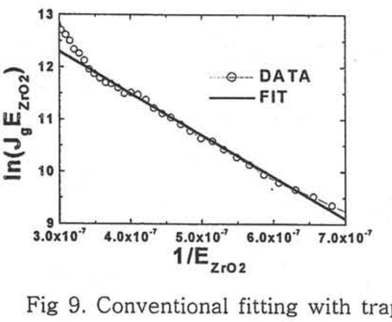


Fig 9. Conventional fitting with trap assisted model

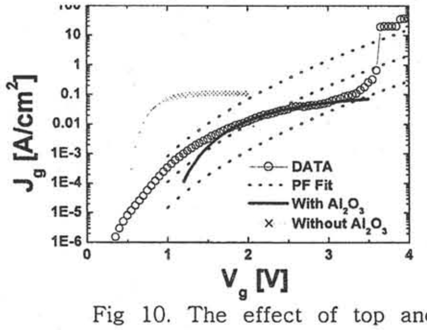


Fig 10. The effect of top and bottom stacked $Al_2O_3$

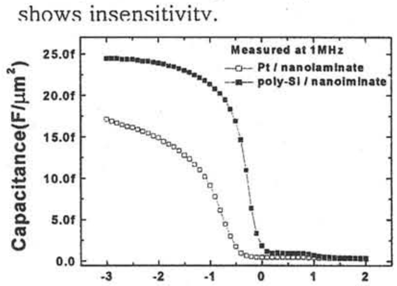


Fig 11.Compatibility of nanolaminate with n+ poly-Si

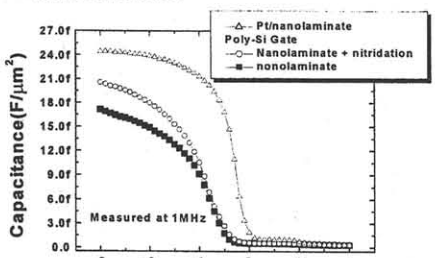


Fig 12. C-V of nitrided nanolaminate with poly-Si & nanolaminate with poly-Si & Pt

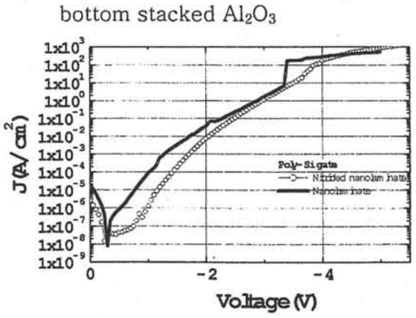


Fig.13 J-V of nanolaminate &nitrided nanolaminate with poly-Si

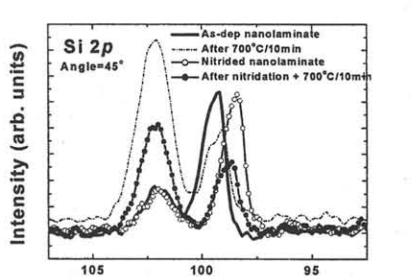


Fig 14. Si2p spectra of nanolaminate with process